22

Elastic Waves

A brief introduction to one-dimensional elasticity theory and elastic wave propagation was given in Section 2.12. In this chapter we will explore the full three-dimensional elasticity equations in the context of elastic wave propagation, or *elastodynamics*. There are many references available on the basic theory of linear and nonlinear elastodynamics (e.g., [6], [11], [141], [249], [255], [367], [422]), though often not in the first-order hyperbolic form we need. In this chapter the equations, eigenstructure, and Riemann solutions are written out in detail for several different variants of the linear problem.

The notation and terminology for these equations differs widely between different fields of application. Much of the emphasis in the literature is on steady-state problems, or *elastostatics*, in which the goal is to determine the deformation of an object and the internal stresses that result from some applied force. These boundary-value problems are often posed as second-order or fourth-order elliptic equations. We will concentrate instead on the hyperbolic nature of the first-order time-dependent problem, and the eigenstructure of this system. This is important in many wave-propagation applications such as seismic modeling in the earth or the study of ultrasound waves propagating through biological tissue. For small deformations, linear elasticity can generally be used. But even this case can be challenging numerically, since most practical problems involve heterogeneous materials and complicated geometry. High-resolution finite volume methods are well suited to these problems, since interfaces between different materials are handled naturally in the process of solving Riemann problems. This has already been explored in one dimension in Section 9.6. These methods can also be extended to nonlinear elasticity equations by incorporating an appropriate nonlinear Riemann solver, allowing the solution of problems with *finite deformations* (meaning larger than infinitesimal), in which case shock waves can form. For even larger deformations plastic behavior is observed, which can also be modeled with hyperbolic systems in some cases. For some examples of the application of hyperbolic theory and Riemann solvers to elastic and elastic–plastic problems, see for example [8], [30], [55], [83], [85], [164], [273], [327], [360], [406], [454], [455], [456]. Here we restrict our attention to linear elastic problems.

Recall from Section 2.12 that there are generally two basic types of waves that can propagate in an elastic solid, P-waves (pressure waves or primary waves) and S-waves (shear waves or secondary waves). In one dimension the P-waves and S-waves can be modeled separately by disjoint systems of two equations each. In multidimensional problems there is a coupling between these modes and the situation is more complicated. However, we

will see that a plane-wave problem in any of the three coordinate directions leads to a system that decouples into the simple structure seen in Section 2.12.4. This means that finite volume methods based on Riemann solvers in the coordinate directions are easy to apply.

22.1 Derivation of the Elasticity Equations

In this section we will informally derive the full three-dimensional elasticity equations. The clear discussion of Davis and Selvadurai [102] has largely motivated the derivation given here, but other derivations and discussion of elastodynamics can be found in many sources, such as those listed above.

We first generalize the notation of Section 2.12.1 from two to three dimensions. The displacement $\vec{\delta}(x, y, z, t)$ now has three components, and $\nabla\vec{\delta}$ is a 3×3 matrix. The strain tensor ϵ is again defined by

$$\epsilon = \frac{1}{2}[\nabla\vec{\delta} + (\nabla\vec{\delta})^T] = \begin{bmatrix} \epsilon^{11} & \epsilon^{12} & \epsilon^{13} \\ \epsilon^{21} & \epsilon^{22} & \epsilon^{23} \\ \epsilon^{31} & \epsilon^{32} & \epsilon^{33} \end{bmatrix}. \tag{22.1}$$

This symmetric matrix has six distinct elements – three extensional strains and three shear strains – given by

$$\begin{aligned} &\epsilon^{11} = \delta^1_x, && \epsilon^{22} = \delta^2_y, && \epsilon^{33} = \delta^3_z \\ &\epsilon^{12} = \tfrac{1}{2}\big(\delta^1_y + \delta^2_x\big), && \epsilon^{13} = \tfrac{1}{2}\big(\delta^1_z + \delta^3_x\big), && \epsilon^{23} = \tfrac{1}{2}\big(\delta^2_z + \delta^3_y\big). \end{aligned} \tag{22.2}$$

The stress tensor σ is also a 3×3 symmetric matrix with six distinct elements,

$$\sigma = \begin{bmatrix} \sigma^{11} & \sigma^{12} & \sigma^{13} \\ \sigma^{21} & \sigma^{22} & \sigma^{23} \\ \sigma^{31} & \sigma^{32} & \sigma^{33} \end{bmatrix}, \tag{22.3}$$

with all elements varying as functions of space and time. This is a tensorial quantity that is written in matrix form corresponding to x–y coordinates. At any point in space this stress tensor represents the internal forces acting at that point. If we introduce a surface through the point with unit normal vector $\vec{n}$, then the traction (force per unit area) acting on this surface is given by the vector $\sigma \cdot \vec{n}$. In particular, the three columns of σ represent the traction acting on planes normal to the x-, y-, and z-axes respectively. Relative to these planes, the components σ^{11}, σ^{22}, and σ^{33} are the *normal stress* components, while σ^{12}, σ^{13}, and σ^{23} are the *shear stress* components. But it is important to keep in mind that for a plane not aligned with the coordinates, the normal and shear stresses relative to that plane will each in general have values that depend on all components of σ.

We can derive a system of conservation laws governing wave motion as a generalization to the systems (2.91) and (2.98) in the one-dimensional case. These equations have the form

$$\begin{aligned}
\epsilon_t^{11} - u_x &= 0,\\
\epsilon_t^{22} - v_y &= 0,\\
\epsilon_t^{33} - w_z &= 0,\\
\epsilon_t^{12} - \frac{1}{2}(v_x + u_y) &= 0,\\
\epsilon_t^{23} - \frac{1}{2}(v_z + w_y) &= 0,\\
\epsilon_t^{13} - \frac{1}{2}(u_z + w_x) &= 0,\\
\rho u_t - \sigma_x^{11} - \sigma_y^{12} - \sigma_z^{13} &= 0,\\
\rho v_t - \sigma_x^{12} - \sigma_y^{22} - \sigma_z^{23} &= 0,\\
\rho w_t - \sigma_x^{13} - \sigma_y^{23} - \sigma_z^{33} &= 0.
\end{aligned} \tag{22.4}$$

The first six equations follow directly from the definition of ϵ in terms of the spatial gradient of $\vec{\delta}$, whereas the velocity (u, v, w) is the time derivative of $\vec{\delta}$. (The first of these was derived in (2.92).) The final three equations in (22.4) express the dynamic relationship between the acceleration and the net force resulting from all the stresses.

The equations (22.4) must be completed by specifying a constitutive stress–strain relationship between σ and ϵ. In general this might be nonlinear, but for small deformations a linear stress–strain relation can be assumed, leading to the multidimensional equations of linear elasticity derived in the next subsection.

22.1.1 Linear Elasticity

For small deformations the stress and strain can be related by a generalization of Hooke's law, which has the general form

$$\sigma^{ij} = \sum_{k,l} C^{ijkl}\epsilon^{kl}. \tag{22.5}$$

The tensor C has 81 components, but by symmetry only 21 are independent. We will make a considerable further simplification by assuming that the material is *isotropic*, and hence the material behavior is the same in any direction. In this case the six independent components of σ can be related to those of ϵ by means of a 6×6 matrix, which will be displayed below.

If we apply a small force σ^{11} in the x-direction to an elastic bar, we expect the material to stretch by a linearly proportional small amount,

$$\epsilon^{11} = \frac{1}{E}\sigma^{11}, \tag{22.6}$$

as in Hooke's law. The parameter E is called *Young's modulus*. In general we also expect the bar to contract slightly in the y- and z-directions as it is stretched in x. Since the material is isotropic, we expect the strains ϵ^{22} and ϵ^{33} to be equal to one another and, for small deformations, linear in ϵ^{11}:

$$\epsilon^{22} = \epsilon^{33} = -\nu\epsilon^{11}.$$

The parameter ν is *Poisson's ratio*. For most materials $0 < \nu < 0.5$, although there are strange materials for which $\nu < 0$ (e.g., [252]). Thermodynamics requires $-1 \le \nu \le 0.5$. If $\nu = 0.5$, then the material is *incompressible*, a mathematical idealization in that in reality any material can be compressed if sufficient force is applied. The assumption $\nu < 0.5$ is required for a hyperbolic formulation.

Using (22.6), we can write

$$\epsilon^{22} = \epsilon^{33} = -\frac{\nu}{E}\sigma^{11}.$$

Similarly, a force applied in the y- or z-direction will also typically cause strains in all three directions. More generally we can think of applying normal stresses σ^{11}, σ^{22}, and σ^{33} simultaneously, resulting in strains that are a linear combination of those obtained from each stress separately. This leads to the extensional strains

$$\begin{aligned}
\epsilon^{11} &= \frac{1}{E}\sigma^{11} - \frac{\nu}{E}\sigma^{22} - \frac{\nu}{E}\sigma^{33}, \\
\epsilon^{22} &= \frac{1}{E}\sigma^{22} - \frac{\nu}{E}\sigma^{11} - \frac{\nu}{E}\sigma^{33}, \\
\epsilon^{33} &= \frac{1}{E}\sigma^{33} - \frac{\nu}{E}\sigma^{11} - \frac{\nu}{E}\sigma^{22}.
\end{aligned} \tag{22.7}$$

The shear strains and shear stresses are related to one another by the simpler relations

$$\sigma^{12} = 2\mu\epsilon^{12}, \quad \sigma^{13} = 2\mu\epsilon^{13}, \quad \sigma^{23} = 2\mu\epsilon^{23}. \tag{22.8}$$

where $\mu \ge 0$ is the *shear modulus*. For elastic materials the shear modulus can be determined in terms of E and ν as

$$\mu = \frac{E}{2(1+\nu)}. \tag{22.9}$$

See [102], for example, for a derivation.

Combining (22.7) and (22.8) gives the desired stress–strain relation

$$\begin{bmatrix} \epsilon^{11} \\ \epsilon^{22} \\ \epsilon^{33} \\ \epsilon^{12} \\ \epsilon^{23} \\ \epsilon^{13} \end{bmatrix} = \begin{bmatrix} 1/E & -\nu/E & -\nu/E & 0 & 0 & 0 \\ -\nu/E & 1/E & -\nu/E & 0 & 0 & 0 \\ -\nu/E & -\nu/E & 1/E & 0 & 0 & 0 \\ 0 & 0 & 0 & 1/2\mu & 0 & 0 \\ 0 & 0 & 0 & 0 & 1/2\mu & 0 \\ 0 & 0 & 0 & 0 & 0 & 1/2\mu \end{bmatrix} \begin{bmatrix} \sigma^{11} \\ \sigma^{22} \\ \sigma^{33} \\ \sigma^{12} \\ \sigma^{23} \\ \sigma^{13} \end{bmatrix}. \quad (22.10)$$

We can invert this matrix to instead determine the stress in terms of the strain,

$$\begin{bmatrix} \sigma^{11} \\ \sigma^{22} \\ \sigma^{33} \\ \sigma^{12} \\ \sigma^{23} \\ \sigma^{13} \end{bmatrix} = \begin{bmatrix} \lambda+2\mu & \lambda & \lambda & 0 & 0 & 0 \\ \lambda & \lambda+2\mu & \lambda & 0 & 0 & 0 \\ \lambda & \lambda & \lambda+2\mu & 0 & 0 & 0 \\ 0 & 0 & 0 & 2\mu & 0 & 0 \\ 0 & 0 & 0 & 0 & 2\mu & 0 \\ 0 & 0 & 0 & 0 & 0 & 2\mu \end{bmatrix} \begin{bmatrix} \epsilon^{11} \\ \epsilon^{22} \\ \epsilon^{33} \\ \epsilon^{12} \\ \epsilon^{23} \\ \epsilon^{13} \end{bmatrix}. \quad (22.11)$$

Here we have introduced the parameter λ defined by

$$\lambda = \frac{\nu E}{(1+\nu)(1-2\nu)}. \quad (22.12)$$

This does not have any direct physical interpretation, but is useful in that it appears in the inverse above. The relation (22.9) has also been used to simplify the form of this inverse. The parameter λ should not be confused with an eigenvalue, for which we use the symbol s in this chapter. The parameters λ and μ are often called the *Lamé parameters* for the material. From (22.9) and (22.12) we can also compute E and ν from λ and μ, as

$$E = \frac{\mu(3\lambda+2\mu)}{\lambda+\mu}, \qquad \nu = \frac{1}{2}\left(\frac{\lambda}{\lambda+\mu}\right). \quad (22.13)$$

The relationship (22.11) can be used to convert (22.4) into a closed system of nine equations for the velocities $\vec{u} = (u, v, w)$ and either σ or ϵ, by eliminating the other set of six parameters (analogously to choosing (2.93) or (2.95) in the one-dimensional case). Either way we obtain a hyperbolic linear system of nine equations. The two alternative systems are similarity transformations of one another and have the same eigenvalues, as they must, since they model the same elastic waves.

We will use $\vec{u}$ and σ, as is more common in linear elasticity. Then we need expressions for the time derivatives of the stresses. These may be obtained by using (22.11) to write, for example,

$$\sigma_t^{11} = (\lambda+2\mu)\epsilon_t^{11} + \lambda\epsilon_t^{22} + \lambda\epsilon_t^{33}$$

and then using the equations of motion (22.4) to evaluate the time derivatives on the right-hand side. We obtain the system

$$\begin{aligned}
\sigma_t^{11} - (\lambda + 2\mu)u_x - \lambda v_y - \lambda w_z &= 0,\\
\sigma_t^{22} - \lambda u_x - (\lambda + 2\mu)v_y - \lambda w_z &= 0,\\
\sigma_t^{33} - \lambda u_x - \lambda v_y - (\lambda + 2\mu)w_z &= 0,\\
\sigma_t^{12} - \mu(v_x + u_y) &= 0,\\
\sigma_t^{23} - \mu(v_z + w_y) &= 0,\\
\sigma_t^{13} - \mu(u_z + w_x) &= 0,\\
\rho u_t - \sigma_x^{11} - \sigma_y^{12} - \sigma_z^{13} &= 0,\\
\rho v_t - \sigma_x^{12} - \sigma_y^{22} - \sigma_z^{23} &= 0,\\
\rho w_t - \sigma_x^{13} - \sigma_y^{23} - \sigma_z^{33} &= 0.
\end{aligned} \tag{22.14}$$

This can be written as

$$q_t + Aq_x + Bq_y + Cq_z = 0, \tag{22.15}$$

with

$$q = \begin{bmatrix} \sigma^{11} \\ \sigma^{22} \\ \sigma^{33} \\ \sigma^{12} \\ \sigma^{23} \\ \sigma^{13} \\ u \\ v \\ w \end{bmatrix}, \qquad A = \begin{bmatrix} 0 & 0 & 0 & 0 & 0 & 0 & -(\lambda+2\mu) & 0 & 0 \\ 0 & 0 & 0 & 0 & 0 & 0 & -\lambda & 0 & 0 \\ 0 & 0 & 0 & 0 & 0 & 0 & -\lambda & 0 & 0 \\ 0 & 0 & 0 & 0 & 0 & 0 & 0 & \mu & 0 \\ 0 & 0 & 0 & 0 & 0 & 0 & 0 & 0 & 0 \\ 0 & 0 & 0 & 0 & 0 & 0 & 0 & 0 & \mu \\ -1/\rho & 0 & 0 & 0 & 0 & 0 & 0 & 0 & 0 \\ 0 & 0 & 0 & -1/\rho & 0 & 0 & 0 & 0 & 0 \\ 0 & 0 & 0 & 0 & 0 & -1/\rho & 0 & 0 & 0 \end{bmatrix}, \tag{22.16}$$

and similar matrices B and C with the nonzero elements shifted to different locations.

The matrices A, B, and C do not commute, and so these equations are generally coupled in the multidimensional case. This is not surprising, since we expect that elastic waves, like acoustic waves, can propagate equally well in any direction. In fact the eigenvalues of $\breve{A} = n^x A + n^y B + n^z C$ are the same for any unit vector $\vec{n}$, and are given by

$$\begin{aligned}
s^1 = -c_p, \quad s^2 = c_p, \quad s^3 = -c_s, \quad s^4 = c_s,\\
s^5 = -c_s, \quad s^6 = c_s, \quad s^7 = s^8 = s^9 = 0.
\end{aligned} \tag{22.17}$$

These are not ordered monotonically, but instead the three eigenvalues with modulus 0 are grouped last, since in practice we only need to propagate six waves after solving any

one-dimensional Riemann problem. The 1- and 2- waves are the P-waves, propagating in the directions $\pm\vec{n}$. There are also two sets of S-waves corresponding to the fact that shear motions are in the two-dimensional plane orthogonal to this direction. The wave speeds are given by

$$c_p = \sqrt{\frac{\lambda + 2\mu}{\rho}}, \qquad c_s = \sqrt{\frac{\mu}{\rho}}. \tag{22.18}$$

The Riemann problem in each coordinate direction is easy to solve. In the x-direction, for example, we have the following eigenvectors of the matrix A of (22.16):

$$r^{1,2} = \begin{bmatrix} \lambda + 2\mu \\ \lambda \\ \lambda \\ 0 \\ 0 \\ 0 \\ \pm c_p \\ 0 \\ 0 \end{bmatrix}, \quad r^{3,4} = \begin{bmatrix} 0 \\ 0 \\ 0 \\ \mu \\ 0 \\ 0 \\ 0 \\ \pm c_s \\ 0 \end{bmatrix}, \quad r^{5,6} = \begin{bmatrix} 0 \\ 0 \\ 0 \\ 0 \\ 0 \\ \mu \\ 0 \\ 0 \\ \pm c_s \end{bmatrix}. \tag{22.19}$$

These correspond to P-waves in x, shear waves with displacement in the y-direction, and shear waves with displacement in the z-direction, respectively. The other three eigenvectors, corresponding to $\lambda^{7,8,9} = 0$, are given by

$$r^7 = \begin{bmatrix} 0 \\ 0 \\ 0 \\ 0 \\ 1 \\ 0 \\ 0 \\ 0 \\ 0 \end{bmatrix}, \quad r^8 = \begin{bmatrix} 0 \\ 1 \\ 0 \\ 0 \\ 0 \\ 0 \\ 0 \\ 0 \\ 0 \end{bmatrix}, \quad r^9 = \begin{bmatrix} 0 \\ 0 \\ 1 \\ 0 \\ 0 \\ 0 \\ 0 \\ 0 \\ 0 \end{bmatrix}. \tag{22.20}$$

These correspond to jumps in σ^{23}, σ^{22}, or σ^{33} alone, each of which causes no wave propagation in x. The matrices B and C have similar eigenvectors, again with the nonzero elements appropriately rearranged.

Note that if we solve a plane-wave problem in which there is only variation in x, then $q_y = q_z = 0$ and the three-dimensional system reduces to $q_t + Aq_x = 0$. In this case the system does decouple into systems of the form discussed in Section 2.12.4. Actually the P-waves given by $r^{1,2}$ in (22.19) carry variation in σ^{22} and σ^{33} as well as in σ^{11} and u. However, this stress in the y- and z-directions exactly balances the stress in x in such a way that the strain is entirely in the x-direction, i.e., $\epsilon^{22} = \epsilon^{33} = 0$, as is clear when the stress components of $r^{1,2}$ are inserted into (22.10). In spite of the fact that the Poisson ratio is typically nonzero, a compressional plane wave in an infinite solid causes no deformation

in the orthogonal directions (as indicated in Figure 2.2). Also, since the second and third columns of A in (22.16) are identically zero, we see that the stresses σ^{22} and σ^{33} cause no dynamic effects and we can drop these variables from the system in deriving the one-dimensional equations (2.93). But note that these one-dimensional equations are based on the assumption of a plane wave in an infinite three-dimensional solid, as discussed further in Section 22.3. Other "one-dimensional" situations lead to different equations. For example, the equations modeling longitudinal waves in thin elastic rod are discussed in Section 22.6.

22.1.2 The Bulk Modulus and Acoustics

The *mean stress* in a solid is defined to be one third the trace of the stress tensor,

$$\frac{1}{3}\,\mathrm{tr}\,(\sigma) = \frac{1}{3}(\sigma^{11} + \sigma^{22} + \sigma^{33}). \tag{22.21}$$

This is an invariant of the stress tensor, i.e., it has the same value regardless of the choice of coordinate system used. The trace of the strain tensor is also an invariant, and this value

$$e \equiv \mathrm{tr}\,(\epsilon) = \epsilon^{11} + \epsilon^{22} + \epsilon^{33}, \tag{22.22}$$

is called the *volumetric strain*. It approximates the relative change in volume in the strained solid. By adding together the three equations of (22.7), we find that

$$e = \frac{1-2\nu}{E}\,\mathrm{tr}\,(\sigma), \tag{22.23}$$

and hence the mean stress is related to the volumetric strain by

$$\frac{1}{3}\,\mathrm{tr}\,(\sigma) = Ke, \tag{22.24}$$

where the *bulk modulus of compressibility* K is defined by

$$K = \frac{E}{3(1-2\nu)} = \lambda + \frac{2}{3}\mu. \tag{22.25}$$

Averaging the first three equations of (22.14) gives an evolution equation for the mean stress,

$$\frac{1}{3}(\sigma^{11} + \sigma^{22} + \sigma^{33})_t - K(u_x + v_y + w_z) = 0. \tag{22.26}$$

We can relate the elastodynamics equations to the acoustics equations derived earlier for gas dynamics if we make the additional assumption on that the stress is *hydrostatic*, as it is in a fluid. This means that there is no shear stress, $\sigma^{12} = \sigma^{13} = \sigma^{23} = 0$, and the extensional stress components are all equal and negative,

$$\sigma^{11} = \sigma^{22} = \sigma^{33} \equiv -p. \tag{22.27}$$

The value p is called the *hydrostatic pressure*, and has the opposite sign from the stresses as discussed in Section 2.12.4. In this case the stress tensor (22.3) reduces to $-pI$ where I is the

identity matrix. Rather than working with this tensor we can reduce the equations and deal only with the scalar pressure p, which satisfies $p = -Ke$ by (22.24), since $p = -\frac{1}{3}\,\mathrm{tr}\,(\sigma)$. The equation (22.26) becomes an evolution equation for the hydrostatic pressure,

$$p_t + K(u_x + v_y + w_z) = 0. \tag{22.28}$$

Since we now also assume that $\sigma^{12} = \sigma^{13} = \sigma^{23} = 0$, we can drop the middle three equations of (22.14) and the final three become

$$\begin{aligned} \rho u_t + p_x &= 0, \\ \rho v_t + p_y &= 0, \\ \rho w_t + p_z &= 0. \end{aligned} \tag{22.29}$$

We recognize (22.28), (22.29) as defining the three-dimensional acoustics equations from Section 18.6. This system has wave speeds given by the "speed of sound"

$$c = \sqrt{\frac{K}{\rho}} = \sqrt{\frac{\lambda + \frac{2}{3}\mu}{\rho}}. \tag{22.30}$$

Note that this is different than the P-wave speed c_p of (22.18), which is the sound speed actually observed in solids. However, since a fluid does not support shear stresses we should set $\mu = 0$, in which case (22.18) and (22.30) do agree. The acoustics equations are sometimes used as an approximate system of equations for modeling P-waves in solids when shear waves are relatively unimportant, particularly in solids where μ is small compared to λ.

22.2 The Plane-Strain Equations of Two-Dimensional Elasticity

We can reduce the three-dimensional equations (22.14) to two space dimensions by setting $q_z \equiv 0$, for example, if we assume there is no variation in the z-direction. Note that the strain $\epsilon^{33} = \delta_z^3$ must be zero in this case, since it is the z-derivative of the z-displacement. (We discuss below when this assumption is reasonable.) The stress σ^{33} will not generally be zero, but can be determined in terms of σ^{11} and σ^{22} as discussed below. Dropping the equation for σ^{33} from (22.14) along with all z-derivative terms, the remaining eight equations reduce to two decoupled systems of equations,

$$\begin{aligned} \sigma_t^{11} - (\lambda + 2\mu)u_x - \lambda v_y &= 0, \\ \sigma_t^{22} - \lambda u_x - (\lambda + 2\mu)v_y &= 0, \\ \sigma_t^{12} - \mu(v_x + u_y) &= 0, \\ \rho u_t - \sigma_x^{11} - \sigma_y^{12} &= 0, \\ \rho v_t - \sigma_x^{12} - \sigma_y^{22} &= 0, \end{aligned} \tag{22.31}$$

and

$$\begin{aligned} \sigma_t^{23} - \mu w_y &= 0, \\ \sigma_t^{13} - \mu w_x &= 0, \\ \rho w_t - \sigma_x^{13} - \sigma_y^{23} &= 0. \end{aligned} \tag{22.32}$$

The latter system (22.32) models shear waves with motion orthogonal to the x–y plane. Waves modeled by this system have speed c_s, the S-wave speed given in (22.18).

The system (22.31) is the more interesting system, and models both P-waves and S-waves for which the motion is in the x–y plane. The S-waves modeled by this system have material motion orthogonal to the direction the wave is propagating, but still within the x–y plane. This system (22.31) is often called the two-dimensional *plane-strain equations*, since the strain is confined entirely to the x–y plane. This is a reasonable model for plane waves propagating through a three-dimensional elastic body in cases where there is no variation in the z-direction, for example, if the x–y plane is a representative slice through a three-dimensional solid with essentially infinite extent in the z-direction, as might occur in modeling large-scale seismic waves in the earth, for example. If it is correct to assume that there is no variation in the z-direction, then it is also valid to assume that $\epsilon^{33} = 0$. Otherwise, if ϵ^{33} had some nonzero value independent of z, then the displacement δ^3 would have to be of the form $\delta^3 = \epsilon^{33}(z - z_0)$ and grow without bound in z. This is not reasonable for finite-amplitude waves. Of course, as the material is compressed in the x- or y-direction it will *try* to expand in z (when $\nu \neq 0$), but it will be prevented from doing so by the adjacent material, which is trying equally hard to expand in the other direction. The result is a nonzero stress σ^{33} while ϵ^{33} remains zero. Indeed, setting $\epsilon^{33} = 0$ in the system (22.11) yields

$$\sigma^{11} = (\lambda + 2\mu)\epsilon^{11} + \lambda\epsilon^{22}, \tag{22.33}$$

$$\sigma^{22} = \lambda\epsilon^{11} + (\lambda + 2\mu)\epsilon^{22}, \tag{22.34}$$

$$\sigma^{33} = \lambda\epsilon^{11} + \lambda\epsilon^{22}. \tag{22.35}$$

The first two equations of this set are all that are needed for the two-dimensional system (22.31), but the stress σ^{33} can also be computed from (22.35) if desired. Alternatively we can obtain

$$\sigma^{33} = \nu(\sigma^{11} + \sigma^{22}) \tag{22.36}$$

from the third equation of (22.7) by setting $\epsilon^{33} = 0$.

Note that if we invert the stress–strain relation (22.33)–(22.35) to find ϵ^{11} and ϵ^{22} in terms of σ^{11} and σ^{22}, we find that

$$\begin{aligned} \hat{E}\epsilon^{11} &= \sigma^{11} - \hat{\nu}\sigma^{22}, \\ \hat{E}\epsilon^{22} &= \sigma^{22} - \hat{\nu}\sigma^{11}, \end{aligned} \tag{22.37}$$

where

$$\hat{E} = \frac{E}{1 - \nu^2}, \qquad \hat{\nu} = \frac{\nu}{1 - \nu}. \tag{22.38}$$

The equations (22.37) have the same form as the three-dimensional stress–strain relations (22.7), but with different effective values for the Young's modulus $\hat{E}$ and Poisson ratio $\hat{\nu}$. These relations can be derived either by inverting the 2×2 system given by (22.33) and (22.34), or from (22.7) by using (22.36).

It is important to note that the plane-strain system (22.31) does *not* in general model elastic waves in a thin plate, in spite of the fact that it might seem natural to view this as a two-dimensional elastic medium. Wave propagation in a plate can be modeled by a two-dimensional hyperbolic system, but (22.31) is not the correct one; see Section 22.5.

We now discuss the eigenstructure of the system (22.31). Rather than displaying the matrices A and B separately in this case, it is more compact and perhaps also more revealing to show the linear combination $\breve{A} = n^x A + n^y B$, where $\vec{n}$ is again a unit vector in an arbitrary direction. The matrix $\breve{A}$ is then the coefficient matrix for the one-dimensional problem modeling the propagation of plane waves in the $\vec{n}$-direction. Setting $\vec{n} = (1, 0)$ or $(0, 1)$ below recovers the matrices A and B separately. We have

$$q = \begin{bmatrix} \sigma^{11} \\ \sigma^{22} \\ \sigma^{12} \\ u \\ v \end{bmatrix}, \qquad \breve{A} = - \begin{bmatrix} 0 & 0 & 0 & n^x(\lambda + 2\mu) & n^y\lambda \\ 0 & 0 & 0 & n^x\lambda & n^y(\lambda + 2\mu) \\ 0 & 0 & 0 & n^y\mu & n^x\mu \\ n^x/\rho & 0 & n^y/\rho & 0 & 0 \\ 0 & n^y/\rho & n^x/\rho & 0 & 0 \end{bmatrix}. \tag{22.39}$$

The eigenvalues of $\breve{A}$ are

$$\breve{s}^1 = -c_p, \quad \breve{s}^2 = c_p, \quad \breve{s}^3 = -c_s, \quad \breve{s}^4 = c_s, \quad \breve{s}^5 = 0, \tag{22.40}$$

where we use s instead of λ to avoid confusion with the Lamé parameter. The P-wave eigenvectors are

$$\breve{r}^1 = \begin{bmatrix} \lambda + 2\mu(n^x)^2 \\ \lambda + 2\mu(n^y)^2 \\ 2\mu n^x n^y \\ n^x c_p \\ n^y c_p \end{bmatrix}, \qquad \breve{r}^2 = \begin{bmatrix} \lambda + 2\mu(n^x)^2 \\ \lambda + 2\mu(n^y)^2 \\ 2\mu n^x n^y \\ -n^x c_p \\ -n^y c_p \end{bmatrix}, \tag{22.41}$$

while the S-wave eigenvectors $r^{3,4}$ and the stationary wave r^5 are

$$\breve{r}^3 = \begin{bmatrix} -2n^x n^y \mu \\ 2n^x n^y \mu \\ [(n^x)^2 - (n^y)^2]\mu \\ -n^y c_s \\ n^x c_s \end{bmatrix}, \qquad \breve{r}^4 = \begin{bmatrix} -2n^x n^y \mu \\ 2n^x n^y \mu \\ [(n^x)^2 - (n^y)^2]\mu \\ n^y c_s \\ -n^x c_s \end{bmatrix}, \qquad \breve{r}^5 = \begin{bmatrix} (n^y)^2 \\ (n^x)^2 \\ -n^x n^y \\ 0 \\ 0 \end{bmatrix}. \tag{22.42}$$

Observe that P-waves $\breve{r}^{1,2}$ have velocity components directed in the $\pm\vec{n}$-direction, the direction in which the plane wave propagates. The S-waves, on the other hand, have motion

in the orthogonal direction $\pm(-n^y, n^x)$. Note also that a P-wave in the x- or y-direction has $\sigma^{12} = 0$, but that a P-wave propagating in any other direction has $\sigma^{12} \neq 0$. This is because the elements of the stress tensor have been expressed in x–y coordinates, and representing a purely extensional stress in some other direction requires all components of σ to be nonzero.

22.3 One-Dimensional Slices

We can reduce the systems of equations (22.31) and (22.32) even further if we assume that there is no variation in the y-direction. As in our discussion of the plane-strain equations above, this is typically valid if we are considering a one-dimensional slice through an essentially infinite medium in cases where there is variation in only one direction (e.g., a plane wave propagating through the earth). It is not a valid model for waves in a "one-dimensional" thin elastic rod, which is discussed in Section 22.6.

Setting all y-derivatives to zero in (22.31) results in the two decoupled systems

$$\begin{aligned} \sigma_t^{11} - (\lambda + 2\mu)u_x &= 0, \\ \rho u_t - \sigma_x^{11} &= 0 \end{aligned} \tag{22.43}$$

and

$$\begin{aligned} \sigma_t^{12} - \mu v_x &= 0, \\ \rho v_t - \sigma_x^{12} &= 0. \end{aligned} \tag{22.44}$$

These are the systems (2.95) and (2.100) introduced in Section 2.12.4. They model P-waves with displacement in x and S-waves with displacement in y, respectively, with wave speeds c_p and c_s given by (22.18).

We have dropped the equation for σ^{22}, which is given by

$$\sigma^{22} = \lambda\epsilon^{11} = \hat{\nu}\sigma^{11}. \tag{22.45}$$

Note that in this case $\sigma^{33} = \sigma^{22}$ by (22.36).

The equations (22.32) reduce to

$$\begin{aligned} \sigma_t^{13} - \mu w_x &= 0, \\ \rho w_t - \sigma_x^{13} &= 0. \end{aligned} \tag{22.46}$$

This system models an independent set of shear waves in which the displacement is in the z-direction rather than in the y-direction (and propagation still in the x-direction).

22.4 Boundary Conditions

Boundary conditions for elastic solids can be imposed in much the same way as for acoustics (see Sections 7.3 and 21.8), but there are now a wider variety of physically meaningful boundary conditions to consider. We will use the two-dimensional plane-strain equations (22.31) for illustration, and consider a point along the left edge of the domain, which we

assume is at $x = 0$. We must then determine ghost-cell values Q_{0j} and $Q_{-1,j}$ based on interior values and the physical boundary conditions. It should be clear how to translate this discussion to other boundaries and to three dimensions.

Periodic or extrapolation boundary conditions are easily imposed, as for other equations, as discussed in Section 21.8. The more interesting cases are where either the motion of the boundary or the traction applied to the boundary is specified. These are discussed in the next two subsections.

22.4.1 Specified Motion

Suppose the velocity of the boundary at $x = 0$, $y = y_j$ is known. Call the velocity at this point (U, V) for brevity. Then following the discussion of Sections 7.3.4 and 21.8.3, we can impose this by specifying the ghost-cell values as follows:

$$\begin{aligned}
\text{for } Q_{0j}: \quad & \sigma^{11}_{0j} = \sigma^{11}_{1j}, && \sigma^{12}_{0j} = \sigma^{12}_{1j}, && \sigma^{22}_{0j} = \sigma^{22}_{1j}, \\
& u_{0j} = 2U - u_{1j}, && v_{0j} = 2V - v_{1j}; && \\
\text{for } Q_{-1,j}: \quad & \sigma^{11}_{-1,j} = \sigma^{11}_{2j}, && \sigma^{12}_{-1,j} = \sigma^{12}_{2j}, && \sigma^{22}_{-1,j} = \sigma^{22}_{2j}, \\
& u_{-1,j} = 2U - u_{2j}, && v_{-1,j} = 2V - v_{2j}. &&
\end{aligned} \tag{22.47}$$

When the Riemann problem is solved at $x = 0$ (i.e., at cell interface $i = 1/2$), this choice insures that the intermediate state $Q^{\Downarrow}_{1/2}$ has velocity (U, V) and satisfies the required physical boundary condition. An important special case is $U = 0$, $V = 0$, in which case the boundary is fixed at this point.

Note that in the case of an elastic solid we must specify both u and v. This differs from two-dimensional acoustics or inviscid fluid dynamics, where only the normal component of velocity is specified as discussed in Sections 21.8.3 and 21.8.4. For an inviscid fluid there can be slip along the boundary, and so the tangential component of velocity cannot be specified. For an elastic solid we must specify both. For a three-dimensional problem we would also have to specify w at the boundary, e.g., $w = 0$ at a fixed boundary. The stresses are not specified and must be free to react as necessary to the imposed motion. This is accomplished by simply reflecting σ from the interior values in (22.47), and the values observed in the resulting Riemann solution $Q^{\Downarrow}_{1/2}$ can be used to obtain the surface traction if this is desired as part of the solution to the problem.

22.4.2 Specified Traction

Often we wish instead to specify the traction at a point on the boundary and compute the resulting motion. At the boundary $x = 0$ this amounts to specifying the values of σ^{11} and σ^{12}, say as $\sigma^{11} = S^{11}$ and $\sigma^{12} = S^{12}$ at the point $x = 0$, $y = y_j$. In particular, if this is a free boundary (the edge of an elastic solid with no external force applied), then we should set $S^{11} = 0$ and $S^{12} = 0$. This is called a *traction-free boundary*. Note that we have no physical control over σ^{22} at this boundary.

The proper ghost cell values for general S^{11} and S^{12} are then given by:

$$\begin{aligned}
&\text{for } Q_{0j}: \quad \sigma^{11}_{0j} = 2S^{11} - \sigma^{11}_{1j}, \quad \sigma^{12}_{0j} = 2S^{12} - \sigma^{12}_{1j}, \quad \sigma^{22}_{0j} = \sigma^{22}_{1j},\\
&\qquad\qquad u_{0j} = u_{1j}, \qquad\qquad v_{0j} = v_{1j};\\
&\text{for } Q_{-1,j}: \quad \sigma^{11}_{-1,j} = 2S^{11} - \sigma^{11}_{2j}, \quad \sigma^{12}_{-1,j} = 2S^{12} - \sigma^{12}_{2j}, \quad \sigma^{22}_{-1,j} = \sigma^{22}_{2j},\\
&\qquad\qquad u_{-1,j} = u_{2j}, \qquad\qquad v_{-1,j} = v_{2j}.
\end{aligned} \tag{22.48}$$

For a three-dimensional problem we would also need to specify $\sigma^{13} = S^{13}$, while σ^{23} and σ^{33} would simply be reflected from the interior, as is done for σ^{22} in (22.48).

22.5 The Plane-Stress Equations and Two-Dimensional Plates

In Section 22.2 we derived a two-dimensional hyperbolic system by using the plane-strain assumption that all displacements are confined to the x–y plane. As discussed there, this is valid if we assume the material is essentially infinite in the z-direction and there is no variation of the solution in that direction. We now consider a different situation, in which the three-dimensional domain is a thin plate bounded by the planes $z = \pm h$ for some small h. We wish to derive two-dimensional equations that model waves whose wavelength is long relative to the thickness of the plate. Each surface of the plate is a free boundary and must be traction-free (see Section 22.4.2), so we have

$$\sigma^{13} \equiv 0, \qquad \sigma^{23} \equiv 0, \qquad \sigma^{33} \equiv 0 \tag{22.49}$$

on the boundary planes $z = \pm h$. To derive a two-dimensional system of equations we will assume that these are identically zero throughout the plate. Then from (22.8) we also have

$$\epsilon^{13} \equiv 0, \qquad \epsilon^{23} \equiv 0. \tag{22.50}$$

Note, however, that we cannot assume $\epsilon^{33} = 0$. Instead, from (22.7) with $\sigma^{33} = 0$ we obtain

$$\epsilon^{33} = -\frac{\nu}{E}(\sigma^{11} + \sigma^{22}), \tag{22.51}$$

along with

$$\begin{aligned}
\epsilon^{11} &= \frac{1}{E}(\sigma^{11} - \nu\sigma^{22}),\\
\epsilon^{22} &= \frac{1}{E}(-\nu\sigma^{11} + \sigma^{22}).
\end{aligned} \tag{22.52}$$

Adding these last two equations together gives

$$\epsilon^{11} + \epsilon^{22} = \frac{1-\nu}{E}(\sigma^{11} + \sigma^{22}). \tag{22.53}$$

Since $\epsilon^{11} + \epsilon^{22} = \delta^1_x + \delta^2_y$ is the x–y divergence of the displacement, we see that if $\epsilon^{11} + \epsilon^{22} \neq 0$, then there is compression or expansion in the x–y plane, and in this case from (22.51) there must be compensating motion in the z-direction whenever the Poisson

ratio ν is nonzero. No matter how thin the plate may appear, it is still three-dimensional, and stretching or compressing it in the x–y plane leads to motion in z of the same order of magnitude.

To derive two-dimensional equations we will assume, however, that σ^{11} and σ^{22}, and hence ϵ^{33}, are independent of z. Recall that $\epsilon^{33} = \delta^3_z$, so $\epsilon^{33} > 0$ corresponds to the plate bulging out, while $\epsilon^{33} < 0$ corresponds to the plate becoming thinner.

As the plate thickens or thins, the z-velocity w must be nonzero. Moreover, it is clearly not valid to assume that the value of w is independent of z. For example, if the plate is bulging out, then we must have $w > 0$ for $0 < z < h$ and $w < 0$ for $-h < z < 0$. Since $w = \delta^3_t$, we have $w_z = \delta^3_{zt} = \epsilon^{33}_t$, and the assumption that ϵ^{33} is independent of z means that w varies linearly in z. Although w is not zero, it is close to zero and symmetric about $z = 0$. The plate equations are most rigorously defined by integrating the three-dimensional equations in z from $-h$ to h and the integral of w then reduces to zero, to leading order. This justifies ignoring the effects of w in deriving the two-dimensional plate equations.

Using the assumptions (22.49) and (22.50) in the system (22.4) gives the following system of equations (after dropping the equations for ϵ^{13}, ϵ^{23}, ϵ^{33}, and w):

$$\begin{aligned}
\epsilon^{11}_t - u_x &= 0,\\
\epsilon^{22}_t - v_y &= 0,\\
\epsilon^{12}_t - \frac{1}{2}(v_x + u_y) &= 0,\\
\rho u_t - \sigma^{11}_x - \sigma^{12}_y &= 0,\\
\rho v_t - \sigma^{12}_x - \sigma^{22}_y &= 0.
\end{aligned} \tag{22.54}$$

To close this system we need the constitutive relations relating σ to ϵ, which are given by (22.52) along with $\sigma^{12} = 2\mu\epsilon^{12}$ coming from (22.8). We can write these either as

$$\begin{aligned}
\epsilon^{11} &= \frac{1}{E}(\sigma^{11} - \nu\sigma^{22}),\\
\epsilon^{22} &= \frac{1}{E}(-\nu\sigma^{11} + \sigma^{22}),\\
\epsilon^{12} &= \frac{1}{2\mu}\sigma^{12}
\end{aligned} \tag{22.55}$$

or, by inverting the system, as

$$\begin{aligned}
\sigma^{11} &= \left(\frac{2\mu}{1-\nu}\right)(\epsilon^{11} + \nu\epsilon^{22}),\\
\sigma^{22} &= \left(\frac{2\mu}{1-\nu}\right)(\nu\epsilon^{11} + \epsilon^{22}),\\
\sigma^{12} &= 2\mu\epsilon^{12}.
\end{aligned} \tag{22.56}$$

As usual, we can eliminate either ϵ or σ from (22.54). If we eliminate ϵ, then we obtain the

system

$$\begin{aligned}
&\sigma_t^{11} - \left(\frac{2\mu}{1-\nu}\right) u_x - \left(\frac{2\mu\nu}{1-\nu}\right) v_y = 0,\\
&\sigma_t^{22} - \left(\frac{2\mu\nu}{1-\nu}\right) u_x - \left(\frac{2\mu}{1-\nu}\right) v_y = 0,\\
&\sigma_t^{12} - \mu(v_x + u_y) = 0,\\
&\rho u_t - \sigma_x^{11} - \sigma_y^{12} = 0,\\
&\rho v_t - \sigma_x^{12} - \sigma_y^{22} = 0.
\end{aligned} \tag{22.57}$$

Note that this system has different coefficients than the plane-strain system (22.31). However, if we define

$$\hat{\lambda} = \frac{2\mu\nu}{1-\nu} = \frac{2\mu\lambda}{\lambda + 2\mu} \tag{22.58}$$

as an effective Lamé parameter for the plate, then

$$\frac{2\mu}{1-\nu} = \hat{\lambda} + 2\mu,$$

and the system (22.57) has exactly the same form as (22.31) but with $\hat{\lambda}$ in place of λ. Hence any method developed for the plane-strain case can also be applied to the plane-stress equations simply by changing the value of λ. In particular, the eigenstructure is the same as that developed in Section 22.2 (with $\hat{\lambda}$ in place of λ), and so we see from the eigenvalues (22.40) that the characteristic wave speeds for waves in a plate are

$$\hat{c}_p = \sqrt{\frac{\hat{\lambda} + 2\mu}{\rho}} = \sqrt{\frac{2\mu}{\rho(1-\nu)}} = \sqrt{\frac{E}{\rho(1-\nu^2)}} \tag{22.59}$$

and

$$c_s = \sqrt{\mu/\rho}, \tag{22.60}$$

respectively. The speed c_s is the usual S-wave speed, but the wave speed $\hat{c}_p$ is smaller than c_p from (22.18) when $0 < \nu < 1/2$, since

$$\hat{\lambda} = \lambda\left(1 - \frac{\nu}{1-\nu}\right) < \lambda. \tag{22.61}$$

We will refer to waves propagating at the velocity $\hat{c}_p$ as *$\hat{P}$-waves*.

Example 22.1. We can investigate wave propagation in a thin plate numerically by solving the three-dimensional elasticity equations in a plate with finite thickness $-h < z < h$ and imposing traction-free boundary conditions $\sigma^{13} = \sigma^{23} = \sigma^{33} = 0$ at $z = \pm h$. To illustrate an isolated $\hat{P}$-wave we can assume the wave is propagating in the x-direction

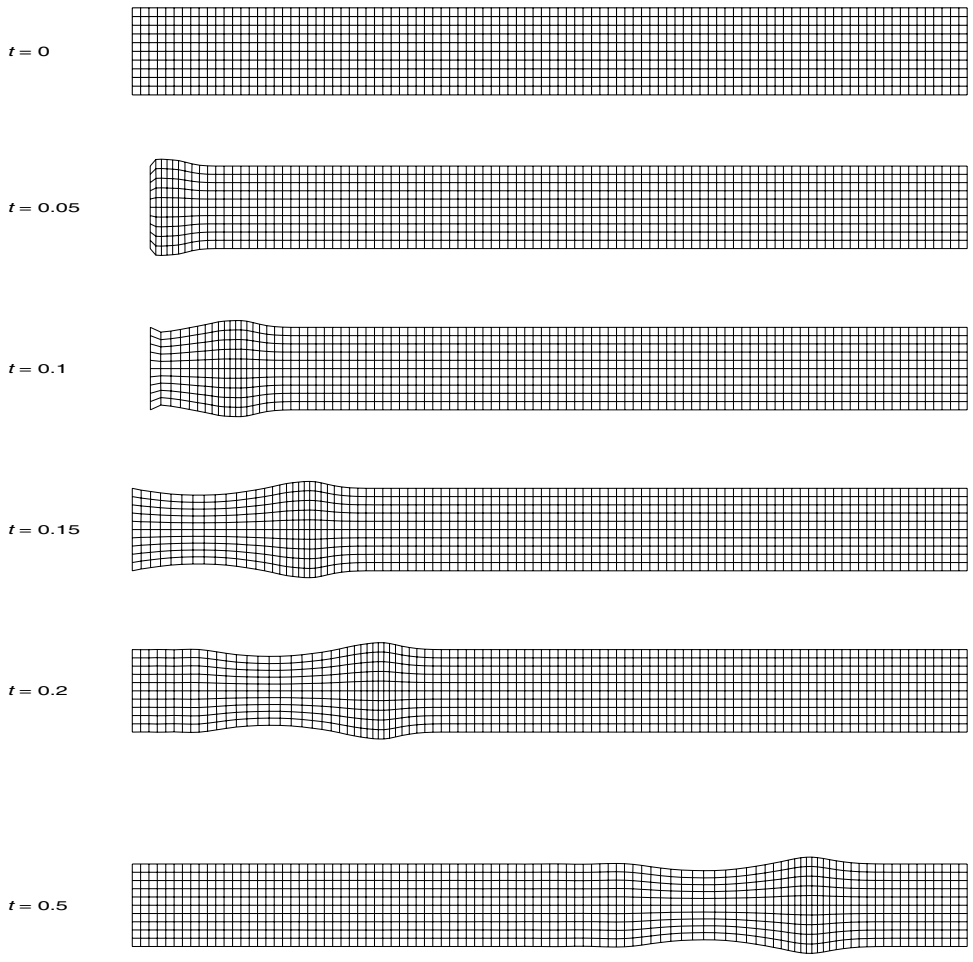

Fig. 22.1. Side view of a thin plate in the x–z plane. The plate is pushed inwards at the left, giving rise to a $\hat{\text{P}}$-wave as described in the text. [claw/book/chap22/plate]

and there is no variation in y, and hence no strain in the y-direction. In this case we can solve a two-dimensional problem in the x–z plane. The appropriate equations are now the plane-strain equations of Section 22.2, rewritten in x and z instead of x and y. Figures 22.1 and 22.2 show results of a numerical calculation in which the traction-free boundary conditions $\sigma^{13} = \sigma^{33} = 0$ are imposed at $z = \pm 0.01$ (see Section 22.4.2) and the plate is initially undisturbed. Boundary conditions at $x = 0$ are given by specifying the velocity (see Section 22.4.1) as

$$\begin{aligned} u(0, z, t) &= \begin{cases} a \sin(2\pi t / T) & \text{if } t \le T, \\ 0 & \text{if } t > T, \end{cases} \\ w(0, z, t) &= 0 \end{aligned} \tag{22.62}$$

with $T = 0.15$. This corresponds to pushing the plate inward and then bringing the edge back to its original location, slowly enough that the wavelength is long relative to the thickness.

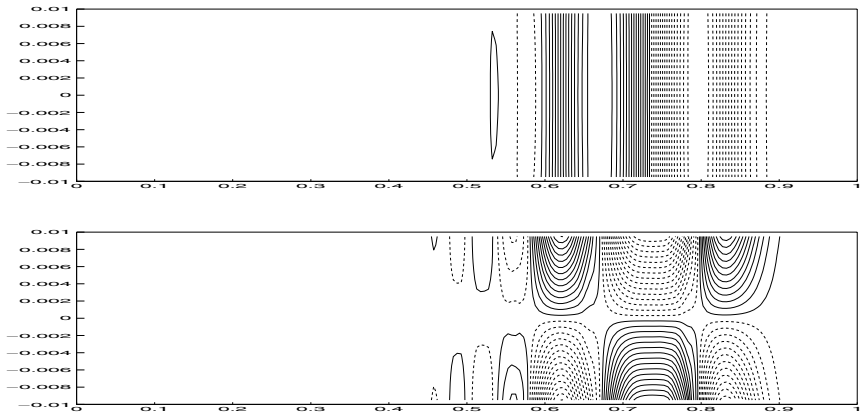

Fig. 22.2. The stress σ^{11} (top) and the vertical velocity w (bottom) at time $t = 0.5$ for the wave-propagation problem shown in Figure 22.1. Contour plots are shown with solid lines for positive values and dashed lines for negative values. `[claw/book/chap22/plate]`

Figure 22.1 shows the deformation of the plate at several times. This deformation has been determined by integrating the velocity (u, w) in each cell over the course of the computation in order to compute the displacement. Points on an initially uniform grid are then displaced by this amount to illustrate the deformed solid. For clarity these deformations are magnified considerably over what is appropriate for linear elasticity (i.e., the constant a in the boundary data (22.62) is taken to be orders of magnitude larger than physically reasonable, but since the equations are linear, the solution simply scales linearly as well). Recall that the computations are always done on a fixed grid in the reference configuration, since the elasticity equations we are considering are written in the Lagrangian frame.

Figure 22.2 shows contours of the computed σ^{11} and w at the final time $t = 0.5$. We see that σ^{11} essentially varies only with x in spite of the fact that the velocity w varies linearly in the z-direction. Moreover we observe that the leading edge of the wave has not yet reached $x = 0.9$ at this time. The material parameters were chosen to be $\rho = 1$, $\lambda = 2$, and $\mu = 1$ so that $c_p = 2$. Rather than traveling at this P-wave speed, the disturbance is propagating at the velocity $\hat{c}_p = \sqrt{3}$, and at time $t = 0.5$ has reached approximately $0.5\hat{c}_p = 0.866$ rather than $0.5c_p = 1$.

If this same computation were repeated but with $u = w = 0$ specified along $z = \pm h$ instead of $\sigma^{13} = \sigma^{33} = 0$ (plane strain rather than a thin plate), the result would look like the figure on the left of Figure 2.2 rather than Figure 22.1, and the disturbance would have reached $x = 1$ at time $t = 0.5$. In this case $w = 0$ would be exactly maintained and there would be no deformation in the z-direction.

It may seem strange that the speed of a $\hat{\text{P}}$-wave in a thin plate is smaller than c_p. After all, the plate is composed of a material characterized by the Lamé parameters λ and μ, and should have a characteristic propagation speed given by c_p. However, a $\hat{\text{P}}$-wave is not simply a P-wave propagating along the plate with deformation confined to the x–y plane. Rather, it is a wave that can be viewed as a superposition of many waves propagating transversely through the plate, bouncing back and forth between the top and bottom surfaces and hence moving at a slower effective speed along the plate. This internal reflection at the

free surface is not apparent in Figure 22.2, since the zig-zagging waves effectively combine into standing waves in the z-direction. In a thicker plate the transverse wave motion would be more apparent. (A similar effect was seen in Section 9.14 for waves propagating in a layered heterogeneous material.)

22.6 A One-Dimensional Rod

Consider a thin elastic rod that is long in the x-direction and has small cross-sectional area, say $-h \le y \le h$ and $-h \le z \le h$. If we consider compressional waves propagating down the rod whose wavelength is long compared to h, then these can be modeled with a one-dimensional system of equations. We can start with the plane-stress equations (22.54), which model a thin plate $-h \le z \le h$, and now restrict also to $-h \le y \le h$ by imposing traction-free boundary conditions on these surfaces: $\sigma^{12} = \sigma^{22} = 0$. As in the derivation of the plane-stress equations, we now assume that in fact $\sigma^{12} = \sigma^{22} = 0$ throughout the rod, and also that $v = 0$ (in addition to the previous assumption that $w = 0$ and $\sigma^{k3} = 0$ for $k = 1, 2, 3$). Then (22.54) reduces to

$$\begin{aligned} \epsilon_t^{11} - u_x &= 0, \\ \rho u_t - \sigma_x^{11} &= 0. \end{aligned} \tag{22.63}$$

From (22.52) we now have the constitutive relation $\epsilon^{11} = \sigma^{11}/E$, and so the one-dimensional system can be rewritten as

$$\begin{aligned} \sigma_t^{11} - E u_x &= 0, \\ \rho u_t - \sigma_x^{11} &= 0. \end{aligned} \tag{22.64}$$

This has the same structure as the equations (22.43) derived for a one-dimensional slice of a three-dimensional solid. But the fact that the rod has traction-free boundaries and is free to contract or expand in y and z leads to a different wave speed,

$$c_p^{\text{rod}} = \sqrt{E/\rho}, \tag{22.65}$$

as seen by computing the eigenvalues of the coefficient matrix from (22.64).

22.7 Two-Dimensional Elasticity in Heterogeneous Media

The multidimensional elastic wave equations can be solved numerically using essentially the same procedure as for the linear acoustics equations, as was described in Chapter 21. This is also easily implemented for a heterogeneous medium by allowing each grid cell to have distinct values for the density ρ and Lamé parameters λ and μ. For the two-dimensional equations discussed in Section 22.2, the Riemann solvers in `[claw/book/chap22/rp]` give an implementation of the necessary eigendecompositions. These are based directly on the eigenstructure determined in Section 22.2. Examples will be presented for the plane-strain case described there, but the same solver work also for the plane-stress equations modeling a thin plate if λ is replaced by $\hat{\lambda}$ as described in Section 22.5.

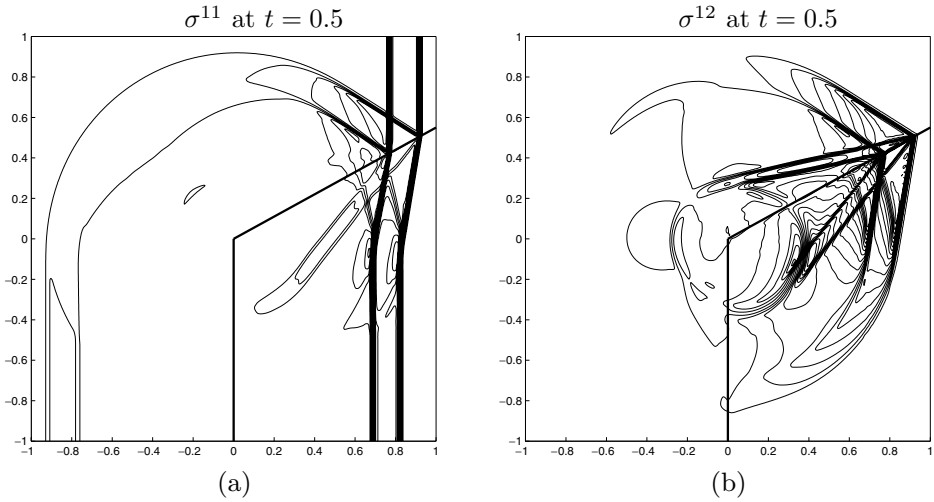

Fig. 22.3. Elastic wave propagation with initial data consisting of a P-wave as shown in Figure 21.1(b): (a) the stress σ^{11}; (b) the shear stress σ^{12}. `[claw/book/chap22/corner]`

Example 22.2. Figure 22.3 shows an example in the same domain indicated in Figure 21.1(a), but with the two regions now containing different elastic materials with parameters

$$\begin{aligned} \rho_l &= 1, & \rho_r &= 1, \\ \lambda_l &= 4, & \lambda_r &= 2, \\ \mu_l &= 0.5, & \mu_r &= 1, \\ c_{pl} &= \sqrt{5} \approx 2.2, & c_{pr} &= 2, \\ c_{sl} &= \sqrt{0.5} \approx 0.7, & c_{sr} &= 1. \end{aligned} \tag{22.66}$$

The initial data is zero everywhere, except for a perturbation as in Figure 21.1(b), in which

$$\sigma^{11} = \lambda_l + 2\mu_l, \quad \sigma^{22} = \lambda_l, \quad \sigma^{12} = 0, \quad u = c_{pl}, \quad v = 0 \tag{22.67}$$

for $-0.35 < x < -0.2$. This is an eigenvector r^2 from (22.41) (with $\vec{n} = (1, 0)$) and hence is a right-going P-wave. After hitting the interface, the transmitted P-wave moves more slowly and there is a partial reflection, as seen in Figure 22.3(a), where a contour plot of σ^{11} is shown. In the elastic case there is also both a transmitted and reflected S-wave along the ramp portion of the interface. These are faintly visible in Figure 22.3(a), since S-waves at an oblique angle have a nonzero σ^{11} component (see Section 22.2). The S-waves are much more clearly visible in Figure 22.3(b), which shows σ^{12}. Note that the transmitted and reflected P-waves also contain significant components of σ^{12}, since they are moving at an angle to the grid.

Example 22.3. As another example of elastic wave propagation in a heterogeneous medium, we consider a wave propagating into a solid that has embedded within it an *inclusion* made out of a stiffer material, as shown in Figure 22.4. The darker region represents material with

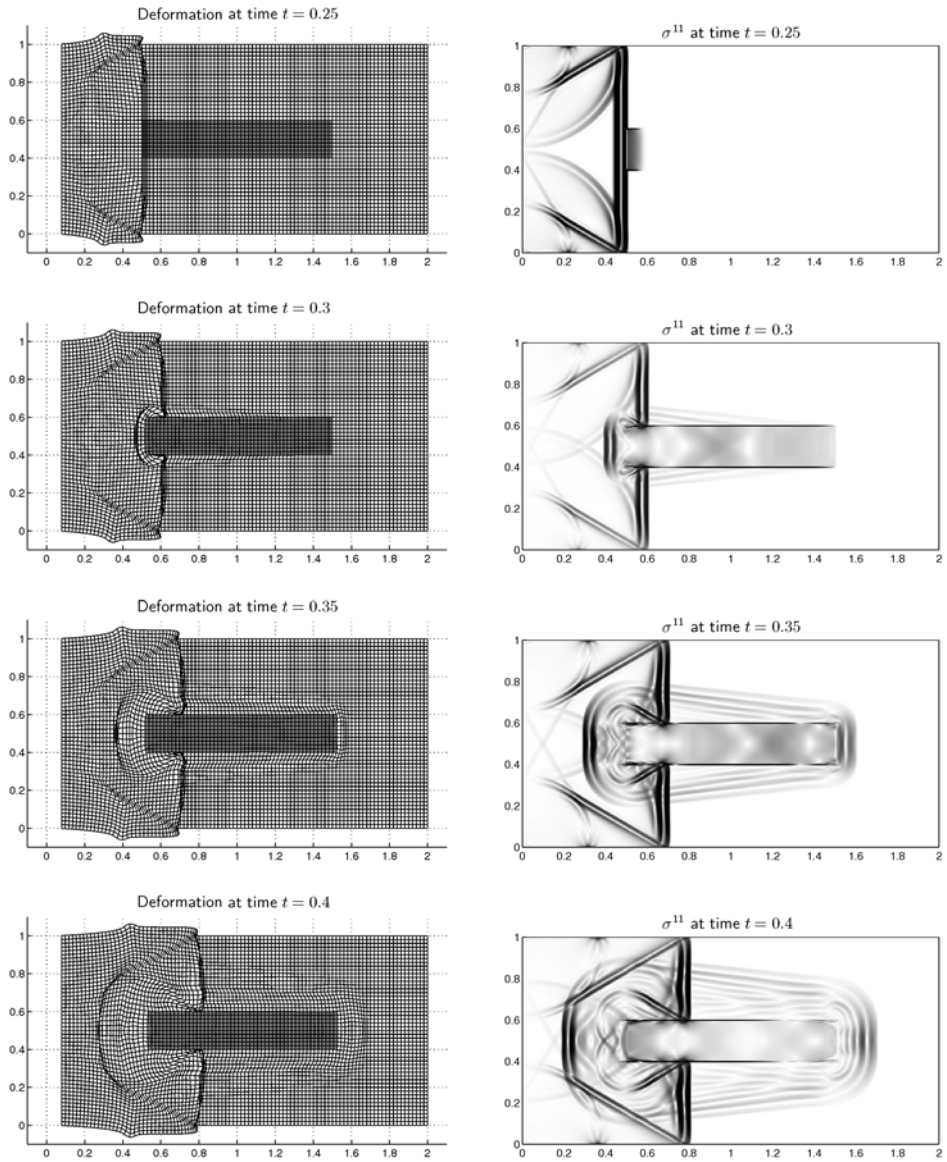

Fig. 22.4. Left column: Deformation of an elastic solid with a stiff inclusion due to compression at the left boundary. The linear deformation is greatly exaggerated. Right column: Schlieren image of σ^{11}. `[claw/book/chap22/inclusion]`

$\lambda = 200$, $\mu = 100$, while the lighter-colored material has $\lambda = 2$ and $\mu = 1$. The density is the same everywhere, $\rho = 1$. The plane-strain equations are solved with traction-free boundary conditions at $y = 0, 1$ and at $x = 1$. At $x = 0$ the velocity is specified as

$$u(0, y, t) = \begin{cases} \epsilon \sin(\pi t/0.025) & \text{if } t < 0.025, \\ 0 & \text{if } t \geq 0.025, \end{cases} \qquad v(0, y, t) = 0. \tag{22.68}$$

The solid is simply pushed over by a small amount at the left boundary. This creates

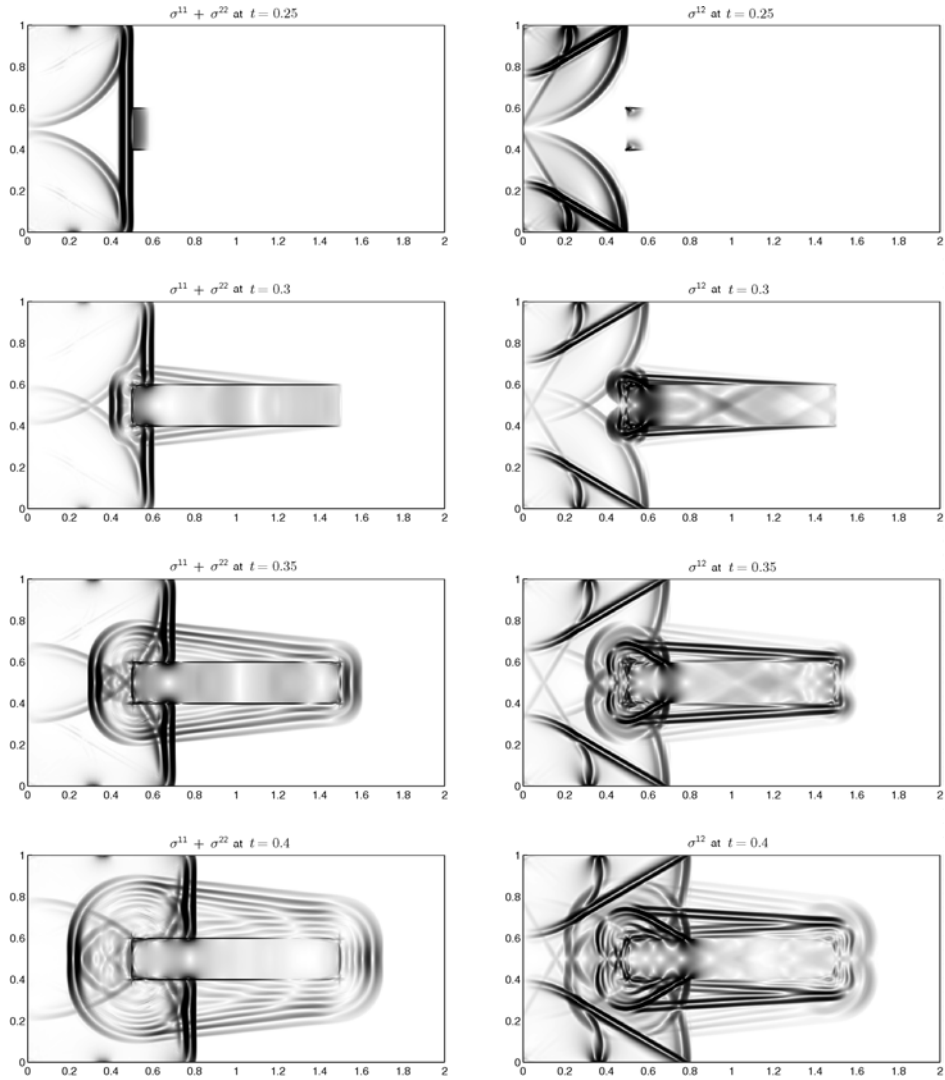

Fig. 22.5. Elastic wave propagation for the example shown in Figure 22.4. Left column: the mean stress $\sigma^{11} + \sigma^{22}$. Right column: the shear stress σ^{12}. `[claw/book/chap22/inclusion]`

a compressional wave, and the resulting wave motion is illustrated in Figure 22.4. The deformation of the solid is computed as described in Example 22.2. Again the displacements shown are much larger than actual linear displacements should be, and have been greatly exaggerated so that they will be visible.

Note that the compression wave is not purely a P-wave, due to its interaction with the free boundaries at $y = \pm 1$. At about $t = 0.25$ the wave hits the inclusion, which is much stiffer and hence tends to be pushed over as a rigid unit. At later times there is very little distortion of the inclusion, which simply shifts over slightly, launching smaller-amplitude waves into the exterior material at the far end and also along its length due to the resistance

to shear. This is not really rigid motion, however. Elastic waves are rapidly bouncing back and forth in the stiff material to accomplish this motion. Note that $c_p = 20$ and $c_s = 10$ in the stiff region, whereas $c_p = 2$ and $c_s = 1$ outside.

Figure 22.5 shows the wave motion more clearly. Here the gradients of $\sigma^{11} + \sigma^{22}$ and σ^{12} are plotted at various times using a *schlieren* image style in which a highly nonlinear color scale is used, so that even very small-amplitude waves show up distinctly. At time $t = 0.25$ we see that waves are just beginning to travel down the stiff inclusion. By time $t = 0.3$ they have reached the far end. As they move along the bar, they launch waves into the surrounding material. The inclusion then begins to vibrate, giving rise to further waves moving vertically away from it.